New Journal of Physics
The open-access journal for physics

Anisotropic mass density by two-dimensional acoustic metamaterials

Daniel Torrent and José Sánchez-Dehesa[1]
Wave Phenomena Group, Department of Electronic Engineering,
Polytechnic University of Valencia, C/Camino de Vera s/n,
E-46022 Valencia, Spain
E-mail: jsdehesa@upvnet.upv.es

New Journal of Physics **10** (2008) 023004 (25pp)
Received 11 September 2007
Published 6 February 2008
Online at http://www.njp.org/
doi:10.1088/1367-2630/10/2/023004

Abstract. We show that specially designed two-dimensional arrangements of full elastic cylinders embedded in a nonviscous fluid or gas define (in the homogenization limit) a new class of acoustic metamaterials characterized by a dynamical effective mass density that is anisotropic. Here, analytic expressions for the dynamical mass density and the effective sound velocity tensors are derived in the long wavelength limit. Both show an explicit dependence on the lattice filling fraction, the elastic properties of cylinders relative to the background, their positions in the unit cell, and their multiple scattering interactions. Several examples of these metamaterials are reported and discussed.

[1] Author to whom any correspondence should be addressed.

Contents

1. Introduction

Recently, there has been great interest in studying the properties of sonic crystals (SC), a name that specifically defines periodic distribution of sound scatterers embedded in a fluid or a gas [1]. Their properties in the low-frequency limit (homogenization) have been studied by several groups in the last few years [2]–[15] for their potential applications as refractive devices. The refractive properties of these systems are controlled by their effective acoustic parameters; i.e. the speed of sound, c_{eff}, and the dynamical mass density ρ_{eff}. The problem of calculating the effective parameters of a heterogeneous medium have been studied in the past [16, 17], but always from a statistical point of view. The underlying periodicity of SC makes it possible to calculate c_{eff} from the acoustic band structure in the low frequency limit by using a plane wave expansion (PWE) [3], but this method does not provide the value of ρ_{eff}. More recently, Mei *et al* [10] working in the framework of multiple scattering theory (MST) were also able to obtain from the acoustic band structures the expressions for both c_{eff} and ρ_{eff}, and claim their validity for any filling fraction. However, we demonstrate here that their expressions are only valid at low volume fractions and coincide with those already obtained by these authors dealing with finite systems [11, 12].

In practical situations, SC are made by clusters with a finite number of cylinders, and therefore their properties in the long wavelength limit have been studied by means of MST without doing any averaging [11, 12, 14]. In other words, each scatterer was considered individually and their positions and mutual interactions into ideal hexagonal and square lattices (isotropic lattices) were fully taken into account. Analytical expressions were obtained for the isotropic mass density and sound velocity as a function of the SC parameters.

In the present work, we go a step further and develop an MST-based procedure to characterize the homogenization of two-dimensional (2D) SC as a function of the positions and elastic properties of a scatterer in the unit cell. We have derived rigorous expressions for the dynamic ρ_{eff} as well for c_{eff} that have been used to design anisotropic acoustic metamaterials

whose properties can be tailored by changing the positions of the scatterers in the unit cell and/or their material constituents.

It is interesting to point out that quite recently Cummer and Schurig [18] have predicted that acoustic cloaking similar to that previously proposed for electromagnetic waves [19, 20] should be possible by means of acoustic materials having anisotropic mass density and sound speed. In this regard, this work demonstrates that acoustic materials with anisotropic parameters are physically realizable. So, in a future work we will look for the recipe to build acoustic materials with the properties shown in [18].

The paper is organized as follows. Section 2 gives a brief introduction to the basic equations of acoustic wave propagation in anisotropic media. In section 3, we summarize the main ingredients of MST that will be used in the following sections. Particularly, we deduce the secular equation from which the homogenization parameters are explicitly obtained.

Afterward, in section 4, the effective parameters are rigorously derived by studying the low frequency limit of the acoustic band structure given by the secular equation. Firstly, the sound speed is analytically derived and an expression is obtained that depends on the so called anisotropy factor of the lattice. Secondly, the well-known expression for effective bulk modulus, B_{eff}, is demonstrated to be hold for the systems. Finally, the anisotropic mass density is also derived from the previously known c_{eff} and B_{eff}. Results for parameters c_{eff} and ρ_{eff} are explicitly calculated for several lattices of rigid cylinders in air. Section 5 reports results for the case in which the elastic properties of cylinders are fully taken into account. The work is summarized in section 6.

2. Anisotropic wave equation

An anisotropic acoustic medium can be characterized by its anisotropic mass density tensor, ρ_{ij}, and the scalar bulk modulus, B [21]. The state equations for the particle velocity vector $\mathbf{v}$ and for the acoustic pressure field P are

$$\frac{\partial P}{\partial x_i} + \sum_j \rho_{ij} \frac{\partial v_j}{\partial t} = 0, \tag{1a}$$

$$\sum_j \frac{\partial v_j}{\partial x_j} + \frac{1}{B}\frac{\partial P}{\partial t} = 0. \tag{1b}$$

As will be seen later, it is worth working with the reciprocal density tensor, so that equations (1) can be cast as:

$$\sum_i \rho_{ki}^{-1} \frac{\partial P}{\partial x_i} + \frac{\partial v_k}{\partial t} = 0, \tag{2}$$

which has been obtained by using the unitary property $\sum_i \rho_{ki}^{-1}\rho_{ij} = \delta_{kj}$.

Now, taking the derivative with respect to x_k and adding in the subindex k

$$\sum_{i,k} \rho_{ki}^{-1} \frac{\partial^2 P}{\partial x_k \partial x_i} + \frac{\partial}{\partial t}\sum_k \frac{\partial v_k}{\partial x_k} = 0. \tag{3}$$

From equation (1*b*) the wave equation for the acoustic pressure is finally obtained:

$$\sum_{i,k} \rho_{ki}^{-1} \frac{\partial^2 P}{\partial x_k \partial x_i} - \frac{1}{B}\frac{\partial^2 P}{\partial t^2} = 0. \tag{4}$$

If we assume plane wave solutions with angular frequency ω:

$$P(\vec{r}, t) = P(\omega)\mathrm{e}^{-\mathrm{i}\mathbf{k}\cdot\mathbf{r}}\mathrm{e}^{\mathrm{i}\omega t}, \tag{5}$$

where $\mathbf{k} = k\cos\theta\hat{\mathbf{x}} + k\sin\theta\hat{\mathbf{y}}$ is the wavenumber. Then, its insertion in equation (4) gives:

$$\left[\rho_{xx}^{-1}\cos^2\theta + \rho_{yy}^{-1}\sin^2\theta + (\rho_{xy}^{-1} + \rho_{yx}^{-1})\sin\theta\cos\theta\right]k^2 - \frac{\omega^2}{B} = 0. \tag{6}$$

And the speed of sound, $c = \omega/k$, is

$$c^2(\theta) = B[\rho_{xx}^{-1}\cos^2\theta + \rho_{yy}^{-1}\sin^2\theta + (\rho_{xy}^{-1} + \rho_{yx}^{-1})\sin\theta\cos\theta], \tag{7}$$

which defines a tensor, c_{ij}, such that

$$c_{ij}^2 = B\rho_{ij}^{-1}, \tag{8}$$

this is the well-known Wood's law [22] generalized to the case of an anisotropic medium.

3. MST

A comprehensive account of MST can be found in textbooks [23] and articles [24, 25]. Therefore, this section briefly reports the basic ingredients to understand the rest of the paper.

Consider a cluster of N parallel cylinders with arbitrary transversal section located at $\vec{R}_\alpha$ (with $\alpha = 1, 2, \ldots, N$) and embedded in an acoustic medium characterized by its sound speed c_b. Let us also assume that an external field, P^{ext}, with frequency ω and wavenumber k impinges the cluster:

$$P^{\mathrm{ext}}(r, \varphi; k) = \sum_q A_q^{\mathrm{ext}} J_q(kr)\mathrm{e}^{\mathrm{i}q\varphi}, \tag{9}$$

where $k = \omega/c_\mathrm{b}$ and (r, φ) are the polar coordinates of an arbitrary point in the 2D space. The total pressure field will be given by $P = P^{\mathrm{sc}} + P^{\mathrm{ext}}$, where P^{sc} is the total scattered field by all the individual α cylinders:

$$P^{\mathrm{sc}}(r, \varphi) = \sum_\alpha \sum_{q=-\infty}^{\infty} (A_\alpha)_q H_q(kr_\alpha)\mathrm{e}^{\mathrm{i}q\varphi_\alpha}, \tag{10}$$

where H_q is the qth order Hankel function of first kind, and $(r_\alpha, \varphi_\alpha)$ are the coordinates with the origin translated to the center of the α-cylinder, i.e. $\vec{r}_\alpha = \vec{r} - \vec{R}_\alpha$, as shown in figure 1. $(A_\alpha)_q$ are the coefficients to be determined.

The total field impinging on the α-cylinder can be expressed by

$$P_\alpha(r_\alpha, \varphi_\alpha; k) = \sum_s (B_\alpha)_s J_s(kr_\alpha)\mathrm{e}^{\mathrm{i}q\varphi_\alpha}, \tag{11}$$

where the coefficients $(B_\alpha)_q$ are related to the $(A_\alpha)_q$ through the T matrix [26]:

$$(A_\alpha)_q = \sum_s (T_\alpha)_{qs}(B_\alpha)_s, \tag{12}$$

being $(T_\alpha)_{qs}$ the elements of the T matrix associated with the α-cylinder. Expressions for the T matrix for a fluid-like cylinder and for an elastic cylinder are known and can be found elsewhere [25, 27].

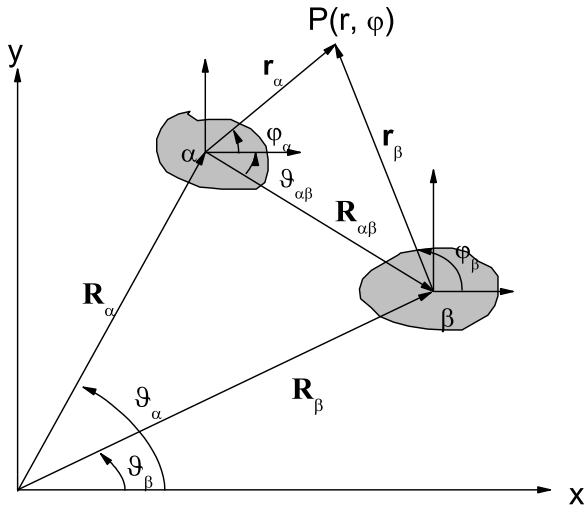

Figure 1. Definition of variables in the multiple scattering algorithm reported in section 3.

After a few manipulations, the solution of the problem is:

$$(A_\alpha)_q = \sum_\beta \sum_r \sum_s (M^{-1}_{\alpha\beta})_{qr} (S_\beta)_{rs} A^{\text{ext}}_s, \tag{13}$$

where

$$(S_\alpha)_{rs} = \sum_q (T_\alpha)_{rq} J_{s-q}(kR_\alpha) \mathrm{e}^{\mathrm{i}(s-q)\vartheta_\alpha}, \tag{14a}$$

$$(M_{\alpha\beta})_{rs} = \delta_{rs}\delta_{\alpha\beta} - (G_{\alpha\beta})_{sr}, \tag{14b}$$

and

$$(G_{\alpha\beta})_{rs} = \sum_q (1-\delta_{\alpha\beta})(T_\alpha)_{rq} H_{q-s}(kR_{\alpha\beta}) \mathrm{e}^{\mathrm{i}(s-q)\vartheta_{\alpha\beta}}. \tag{15}$$

3.1. Band structure calculation

If the cylinders are ordered in a 2D lattice, their α-positions are defined by the Bravais lattice $\mathbf{R}_\alpha = n_1\mathbf{a}_1 + n_2\mathbf{a}_2$, where n_1 and n_2 are integers and $\mathbf{a}_1$ and $\mathbf{a}_2$ are the primitive vectors:

$$\mathbf{a}_1 = a_1\hat{\mathbf{x}} \equiv a\hat{\mathbf{x}}, \tag{16a}$$

$$\mathbf{a}_2 = a_2\cos\phi\hat{\mathbf{x}} + a_2\sin\phi\hat{\mathbf{y}}. \tag{16b}$$

Bloch theorem relates the A-coefficients at any arbitrary α-site with those corresponding to the cylinder at the origin of coordinates:

$$(A_\alpha)_q = \mathrm{e}^{\mathrm{i}\mathbf{K}\cdot\mathbf{R}_\alpha}(A_0)_q, \tag{17}$$

where $\mathbf{K}$ is a Bloch wavenumber. This relationship applied to (13) allows to obtain:

$$(A_0)_r - \sum_s (A_0)_s \tilde{G}_{rs} = (S_0)_{rs} A^{\text{ext}}_s, \tag{18}$$

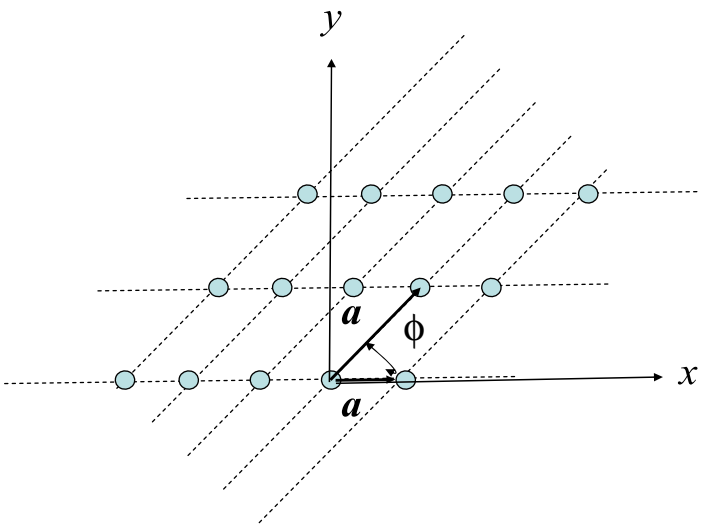

Figure 2. General lattice in the 2D space. $\mathbf{a_1}$ and $\mathbf{a_2}$ represent the primitive lattice vectors and ϕ is the angle between them.

where

$$\tilde{G}_{rs} = \sum_q T_{rq} \sum_{\beta\neq 0} \mathrm{e}^{\mathrm{i}\mathbf{K}\cdot\mathbf{R}_\beta} H_{q-s}(kR_{0\beta})\mathrm{e}^{\mathrm{i}(s-q)\vartheta_{0\beta}} \tag{19}$$

has been obtained by considering that all cylinders are equal (i.e. $T_\alpha = T;\ \forall\alpha$). Also, it can be cast in terms of sums in the reciprocal lattice by using the method developed in [28]:

$$\sum_{\beta\neq 0} \mathrm{e}^{\mathrm{i}\mathbf{K}\cdot\mathbf{R}_\beta} H_{q-s}(kR_{0\beta})\mathrm{e}^{\mathrm{i}(s-q)\vartheta_{0\beta}} = (-1)^{s-q} S^{\mathrm{H}}_{s-q}(k,\mathbf{K}), \tag{20}$$

where

$$S^{\mathrm{H}}_l(k,\mathbf{K}) = S^J_l(k,\mathbf{K}) + \mathrm{i}S^Y_l(k,\mathbf{K}), \tag{21a}$$

$$S^J_l(k,\mathbf{K}) = -\delta_{l0}, \tag{21b}$$

$$S^Y_l(k,\mathbf{K})J_{l+1}(kR_{\min}) = -\left[Y_l(kR_{\min}) + \frac{2}{\pi kR_{\min}}\right]\delta_{l0} - 4\mathrm{i}^l \frac{k}{V_{\mathrm{d}}} \sum_h \frac{J_{l+1}(G_hR_{\min})}{G_h(G_h^2-k^2)}\mathrm{e}^{\mathrm{i}l\theta_h}. \tag{21c}$$

In these expressions, $\mathbf{G}_h = \mathbf{K} + h_1\mathbf{b}_1 + h_2\mathbf{b}_2$ is a vector (in the reciprocal space) obtained by the translation of primitive reciprocal lattice vectors $\mathbf{b}_1$ and $\mathbf{b}_2$ and adding the Bloch wavevector $\mathbf{K}$. V_{d} is the area of the 2D unit cell ($V_{\mathrm{d}} = |\mathbf{a}_1 \times \mathbf{a}_2|$ in figure 2) and $R_{\min}$ is the smaller distance between corners of the unit cell.

With no external field ($A^{\mathrm{ext}} = 0$), the equation (18) becomes

$$A_r - \sum_{rs} T_{rq}(k) S^{\mathrm{H}}_{s-q}(k,\mathbf{K}) A_s = 0, \tag{22}$$

where the subindex 0 has been omitted for simplification. This is a set of coupled linear equations that in matrix form is $\mathcal{M}\cdot\mathcal{A} = 0$, the elements of the M matrix are:

$$M_{rs} = \delta_{rs} - \sum_q T_{rq}(k) S^{\mathrm{H}}_{s-q}. \tag{23}$$

The solution of the secular equation $\det\mathcal{M} = 0$ determines the acoustic bands $\mathbf{K}(\omega)$.

4. Effective parameters for lattices of rigid cylinders

In what follows, we present a rigorous derivation of the effective parameters for the general case of lattice cylinders embedded in a nonviscous liquid or a gas. The theory developed here is valid for all kind of material cylinders: rigid, fluidlike and full elastic cylinders. Firstly, the effective speed of sound is obtained by studying the low frequency limit of acoustic bands. Then, the effective bulk modulus is obtained from T_{00}, the first diagonal element of the T matrix corresponding to a cluster that is anisotropic. Finally, the anisotropic effective mass density is obtained from the relation $c_{\text{eff}}^2 = B_{\text{eff}}/\rho_{\text{eff}}$.

In practical applications the condition of rigid cylinders (i.e. $\rho \approx \infty$) is the common situation encountered when working with solid cylinders (made of, for example, metals like lead, iron or aluminium) embedded in air. So, in this section, we present a comprehensive analysis of results for this particular case and results for elastic cylinders will be studied in section 5.

4.1. Effective speed of sound

In the long wavelength limit, $k \to 0$ (i.e. $\omega \to 0$), the dispersion relation, $\mathbf{K}(\omega)$, for sound waves propagating in a periodic medium becomes linear and an effective speed of sound can be obtained from $c_{\text{eff}} = \lim_{\omega\to 0}(\omega/|\mathbf{K}(\omega)|)$, which can also be cast as:

$$\overline{c}_{\text{eff}} = \lim_{k\to 0} \frac{k}{|\mathbf{K}(k)|}, \tag{24}$$

where $\overline{c}_{\text{eff}} = c_{\text{eff}}/c_{\text{b}}$ is the effective speed of sound relative to that of the background. Hereafter, an overlined variable will be used to denote the corresponding quantity normalized to that of the background. Moreover, k is the wavevector in the embedded background; i.e. $k = |\mathbf{k}| = \omega/c_{\text{b}}$ and $\mathbf{K}(k) = K\cos\theta\hat{\mathbf{x}} + K\sin\theta\hat{\mathbf{y}}$ (θ being the polar angle defined by $\mathbf{K}$).

To study this limit, it is convenient to define frequency-normalized coefficients $\hat{A}_q$ such that

$$A_q(k) \equiv \hat{A}_q(k) k^{-|q|-\delta_{0q}}. \tag{25}$$

Here, we are dealing with lattices of circular-shaped cylinders, which have diagonal T matrices. Then, the equation for coefficients $\hat{A}_q$ is

$$\hat{A}_q - T_q \sum_s S^{\text{H}}_{s-q} k^{|s|+\delta_{s0}-|q|-\delta_{q0}} \hat{A}_s = 0 \tag{26}$$

and we obtain for the M matrix:

$$M_{qs} = \delta_{qs} - T_q S^{\text{H}}_{s-q}\, k^{|s|+\delta_{s0}-|q|-\delta_{q0}}. \tag{27}$$

It was shown in [15] that the T matrix elements for both the elastic and the fluid-like cylinders have the same asymptotic form at large wavelengths. In fact, the elements can be given (in the low frequency limit) as a function of quantities $\hat{T}_q$ that are independent of k:

$$T_q(k) \equiv \hat{T}_q\, k^{2|q|+2\delta_{q0}}. \tag{28}$$

In this limit $T_q S^{\text{H}}_{s-q} k^{|s|+\delta_{s0}-|q|-\delta_{q0}} \approx \mathrm{i}\hat{T}_q S^{Y}_{l} k^{|s|+|q|+\delta_{s0}+\delta_{q0}}$ and, therefore, the dispersion relation is determined from:

$$\det \hat{\mathcal{M}} = 0, \tag{29}$$

where the matrix elements of $\hat{\mathcal{M}}$ are

$$\hat{M}_{qs} = \delta_{qs} - \mathrm{i}\hat{T}_q \lim_{k\to 0} S^Y_{s-q} k^{|s|+|q|+\delta_{s0}+\delta_{q0}}. \tag{30}$$

The secular equation (29) can be solved only numerically. The dimension of $\hat{\mathcal{M}}$ is determined by the truncation on the angular momenta needed to get convergence. For $|q| \leqslant Q_{\max}$ and $|s| \leqslant Q_{\max}$, the dimension of $\hat{\mathcal{M}}$ is $(2Q_{\max}+1)\times(2Q_{\max}+1)$. Therefore, the calculation of the dispersion relation is not an easy task and to obtain an analytical expression for $c_{\mathrm{eff}}(k)$ is impossible if one follows this solving procedure. However, appendix B shows that there exists a block matrix of dimension 3×3 containing only the dependence on $\bar{c}_{\mathrm{eff}}$. Also, it is demonstrated that solving $\det(A - BD^{-1}C) = 0$ is equivalent to solving $\det\hat{\mathcal{M}} = 0$. $A - BD^{-1}C$ is the following 3×3 matrix:

$$A - BD^{-1}C = \begin{pmatrix} \Delta - \eta\dfrac{\bar{c}^2_{\mathrm{eff}}}{1-\bar{c}^2_{\mathrm{eff}}} f & \mathrm{i}\eta\dfrac{\bar{c}_{\mathrm{eff}}}{1-\bar{c}^2_{\mathrm{eff}}} f & \eta\dfrac{1}{1-\bar{c}^2_{\mathrm{eff}}} f + \Gamma \mathrm{e}^{2\mathrm{i}\theta} \\ -\mathrm{i}\zeta\dfrac{\bar{c}_{\mathrm{eff}}}{1-\bar{c}^2_{\mathrm{eff}}} f & 1-\zeta\dfrac{\bar{c}^2_{\mathrm{eff}}}{1-\bar{c}^2_{\mathrm{eff}}} f & \mathrm{i}\zeta\dfrac{\bar{c}_{\mathrm{eff}}}{1-\bar{c}^2_{\mathrm{eff}}} f \\ \eta\dfrac{1}{1-\bar{c}^2_{\mathrm{eff}}} f + \Gamma^* \mathrm{e}^{-2\mathrm{i}\theta} & -\mathrm{i}\eta\dfrac{\bar{c}_{\mathrm{eff}}}{1-\bar{c}^2_{\mathrm{eff}}} f & \Delta^* - \eta\dfrac{\bar{c}^2_{\mathrm{eff}}}{1-\bar{c}^2_{\mathrm{eff}}} f \end{pmatrix}. \tag{31}$$

The secular equation associated with this matrix can be analytically solved for $\bar{c}^2_{\mathrm{eff}}$:

$$\bar{c}^2_{\mathrm{eff}} = \frac{|\Delta|^2 - |\Gamma|^2 - f^2\eta^2 - 2f\eta|\Gamma|\cos\Phi_\Gamma\cos 2\theta + 2f\eta|\Gamma|\sin\Phi_\Gamma\sin 2\theta}{(1+f\zeta)\left[(\Delta+f\eta)(\Delta^*+f\eta) - |\Gamma|^2\right]}. \tag{32}$$

It is important to remember that Δ and Γ contains lattice sums on the reciprocal space. These quantities as well as the rest of the variables in the expressions above are fully described in appendix B.

Note that the expression for $\bar{c}^2_{\mathrm{eff}}$ takes the form of an angle-dependent speed of sound in an anisotropic medium,

$$\bar{c}^2_{\mathrm{eff}}(\theta) = \bar{c}^2_{s+} + \bar{c}^2_{s-}\cos 2\theta + \bar{c}_{a+}\sin 2\theta, \tag{33}$$

where the components of the velocity tensor are

$$\bar{c}^2_{s+} = \frac{|\Delta|^2 - |\Gamma|^2 - f^2\eta^2}{(1+f\zeta)\left[(\Delta+f\eta)(\Delta^*+f\eta) - |\Gamma|^2\right]}, \tag{34a}$$

$$\bar{c}^2_{s-} = -\frac{2f\eta|\Gamma|\cos\Phi_\Gamma}{(1+f\zeta)\left[(\Delta+f\eta)(\Delta^*+f\eta) - |\Gamma|^2\right]}, \tag{34b}$$

$$\bar{c}^2_{a+} = \frac{2f\eta|\Gamma|\sin\Phi_\Gamma}{(1+f\zeta)\left[(\Delta+f\eta)(\Delta^*+f\eta) - |\Gamma|^2\right]}. \tag{34c}$$

An alternative expression is

$$\bar{c}^2_{\mathrm{eff}}(\theta) = \bar{c}^2_{xx}\cos^2\theta + \bar{c}^2_{yy}\sin^2\theta + (\bar{c}^2_{xy} + \bar{c}^2_{yx})\sin\theta\cos\theta, \tag{35}$$

where

$$\bar{c}^2_{xx} = \bar{c}^2_{s+} + \bar{c}^2_{s-}, \tag{36a}$$

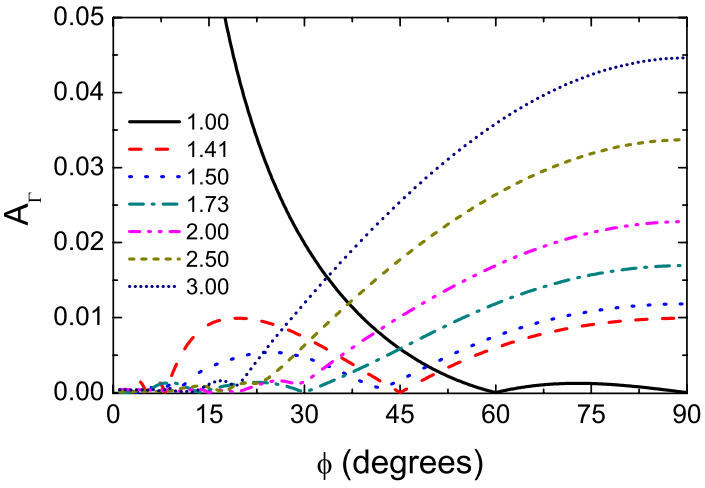

Figure 3. Anisotropy factor, A_Γ, which is defined in (37), for several values of the ratio, a_2/a_1, as a function of the angle, ϕ, between lattice vectors. Anisotropy disappears for the 2D isotropic lattices (square and hexagonal) corresponding to the parameters described in table 1.

Table 1. Effective properties of several 2D topologies studied here. a denotes the length of the smaller primitive translation vectors of the corresponding lattice (see figure 2).

Primitive basis	Topology	Symmetric
$a_2 = a_1 = a;\ \phi = 60^\circ$	Hexagonal	Yes
$a_2 = a_1 = a;\ \phi = 90^\circ$	Square	Yes
$a_2 = \sqrt{2}a_1 = \sqrt{2}a;\ \phi = 45^\circ$	Square	Yes
$a_2 = \sqrt{3}a_1 = \sqrt{3}a;\ \phi = 30^\circ$	Hexagonal	Yes

$$\overline{c}^2_{yy} = \overline{c}^2_{s+} - \overline{c}^2_{s-}, \tag{36b}$$

$$\overline{c}^2_{yx} = \overline{c}^2_{xy} = \overline{c}^2_{a+}. \tag{36c}$$

We see that anisotropy in (32) and (33) comes from factor Γ. In factor Γ, which is given in (B.39), the main contribution to the anisotropy comes from $\Gamma^{(0)}$ (see (B.20)). The value of $\Gamma^{(0)}$ given in (B.20) allows to introduce the so called parameter of anisotropic strength A_Γ, which is defined as:

$$A_\Gamma \equiv \left| \sum_{h\neq 0} \frac{J_3(G_h R_{\min})}{G_h^3 R_{\min}^3} \mathrm{e}^{-2\mathrm{i}\theta_h} \right|. \tag{37}$$

Figure 3 plots A_Γ for several values of the ratio a_2/a_1 as a function of the angle between lattice vectors. The calculations of A_Γ predicts that large anisotropy in sound speed and mass density should be expected for the lattices where this factor takes large values. The predictions are corroborated by the results obtained for c_{eff} and ρ_{eff} as is shown below.

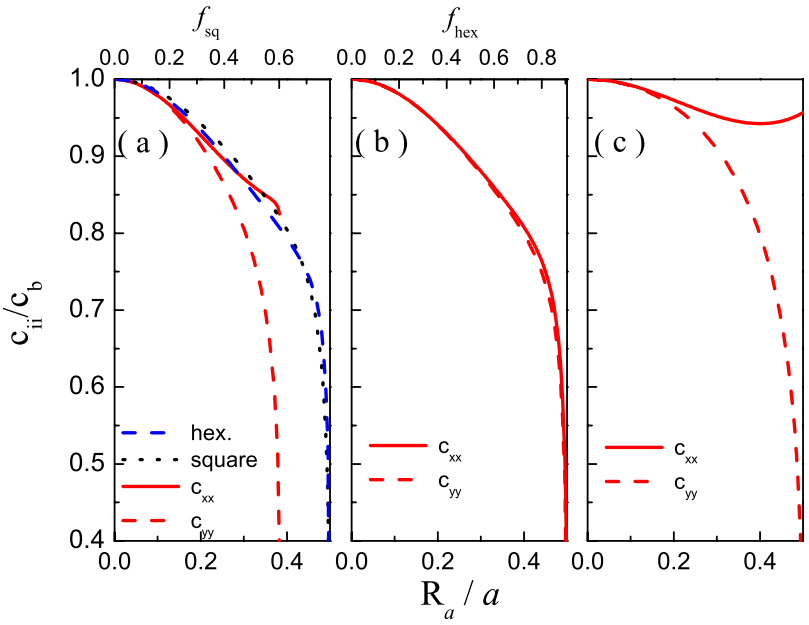

Figure 4. Diagonal components of the speed of sound tensor, $\sqrt{(c_{ii}/c_{\mathrm{b}})^2}$ as a function of the cylinder radius, R_a for the three anisotropic lattices: (a) $a_2 = a_1$, $\phi = 45^\circ$; (b) $a_2 = a_1$, $\phi = 75^\circ$ and (c) $a_2 = 2a_1$, $\phi = 75^\circ$. Results for the isotropic lattices (hexagonal and square) are also depicted in (a) for comparison. The filling fraction f for the square (sq) and hexagonal (hex) lattices are also shown to emphasize that f is determined by R_a and the symmetry of the lattice.

The strength of anisotropic effects predicted by A_Γ is analyzed in figure 4, where the diagonal elements of the sound speed tensor, $\sqrt{\bar{c}_{xx}^2}$ and $\sqrt{\bar{c}_{yy}^2}$, are plotted for the case of rigid cylinders in three different anisotropic lattices and compared with the corresponding results for the hexagonal lattice, which is isotropic. Note that the maximum possible value for R_a, which is determined by the touching condition between neighboring cylinders, depends on the lattice geometry. It is seen in figure 4 that the more anisotropic behavior corresponds to the case $a_2 = 2a_1$ and $\phi = 75^\circ$, which has the larger value of A_Γ (see figure 3).

4.1.1. Isotropic lattices. The case of isotropic lattices deserves special attention because results has been published by two different research teams [3, 10]. The solution for this case is easily obtained from matrix (31) by introducing the isotropy condition, that is $\Gamma = 0$. After straightforward manipulations, the secular equation can be cast as:

$$\det \begin{vmatrix} \Delta - \eta \dfrac{\bar{c}_{\mathrm{eff}}^2}{1-\bar{c}_{\mathrm{eff}}^2} f & \mathrm{i}\eta \dfrac{\bar{c}_{\mathrm{eff}}}{1-\bar{c}_{\mathrm{eff}}^2} f & \eta \dfrac{1}{1-\bar{c}_{\mathrm{eff}}^2} f \\ -\mathrm{i}\zeta \dfrac{\bar{c}_{\mathrm{eff}}}{1-\bar{c}_{\mathrm{eff}}^2} f & 1-\zeta \dfrac{\bar{c}_{\mathrm{eff}}^2}{1-\bar{c}_{\mathrm{eff}}^2} f & \mathrm{i}\zeta \dfrac{\bar{c}_{\mathrm{eff}}}{1-\bar{c}_{\mathrm{eff}}^2} f \\ \eta \dfrac{1}{1-\bar{c}_{\mathrm{eff}}^2} f & -\mathrm{i}\eta \dfrac{\bar{c}_{\mathrm{eff}}}{1-\bar{c}_{\mathrm{eff}}^2} f & \Delta - \eta \dfrac{\bar{c}_{\mathrm{eff}}^2}{1-\bar{c}_{\mathrm{eff}}^2} f \end{vmatrix} = 0. \tag{38}$$

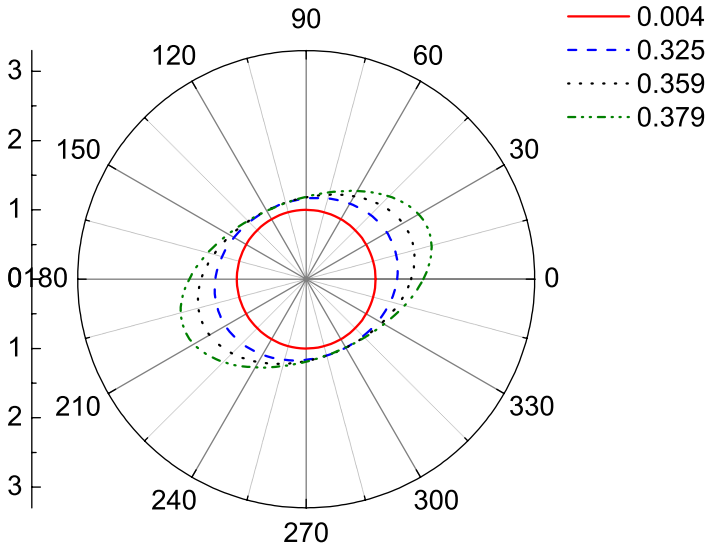

Figure 5. Index ellipsoid $n_{\text{eff}}(\theta)$ for the anisotropic lattice defined by $a_2 = a_1$ and $\phi = 45^\circ$ (see figure 2) for several values of cylinder radius in reduced units, R_a/a. Note that the ellipsoid longer axis follows the direction that bisects the angle $\phi = 22.5^\circ$.

The analytical solution of this equation is:

$$\bar{c}^2_{\text{eff}} = \frac{\Delta - f\eta}{\Delta + f\eta} \cdot \frac{1}{1 + f\zeta}. \tag{39}$$

This solution contains relevant terms of multiple scattering interaction that has been forgotten in the solution given by Mei *et al* [10], who were also working in the framework of MST. Particularly, our results reduced to those in [10] when we impose in (39) the condition $\Delta = 1$. In other words, when it is assumed that multiple scattering interactions are neglected. In fact, it has been shown by us [11, 12] that this condition is only valid at low filling fractions. The parameter Δ is responsible for the abrupt decrease of speed of sound when the filling fraction approaches the condition of close-packing as shown in figure 4. This behavior is not shown in figure 1 of [10]. Our results fully agree with those found in Krokhin *et al*, which used a PWE (see figure 1 in [3]).

4.1.2. Wave propagation. The sound propagation through anisotropic lattices has its own interest and will be discussed in a separate paper, which will be published elsewhere. However, it is possible to advance the behavior expected by simply looking at the so called refractive index ellipsoid, which we have introduced here in acoustics in a manner similar to that in optics:

$$n_{\text{eff}}(\theta) = \frac{1}{\sqrt{c^2_{\text{eff}}(\theta)}}. \tag{40}$$

Two index ellipsoids have been plotted in polar coordinates in figures 5 and 6 for two different anisotropic lattices and for several values of cylinder radius R_a. In figure 5 it should be noted that the principal axes are rotated 22.5° with respect to the x-axis of the lattice. However, it is remarkable how the principal axes are slightly rotated with respect to the xy-axis for the

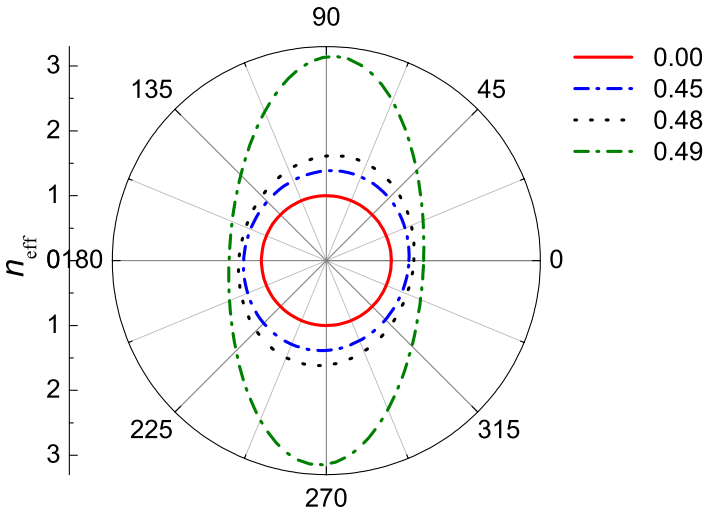

Figure 6. Index ellipsoid $n_{\text{eff}}(\theta)$ for the anisotropic lattice defined by $a_2 = 2a_1$ and $\phi = 30^\circ$ and for several cylinder radius R_a. Note how the rotation of the principal axis depends on R_a (i.e. it is a function of the lattice filling fraction).

lattice studied in figure 5, and more important is the tilted angle which depends on the filling fraction of the lattice. The wave propagation will respond to the index ellipsoid, in such a way that slow propagation is expected along the direction defined by the longer side of the ellipsoid and faster propagation will take place along the direction defined by the smaller side of the ellipsoid.

4.2. Effective bulk modulus

The effective parameters of a cluster of cylinders in which the underlying lattice is isotropic (hexagonal or square) were obtained in [12] from the scattered field by the given cluster. In brief, the method associates to the cluster an effective T matrix, T_{eff}, and assumes that (in the long wavelength limit) this matrix must be equal to that of a homogeneous isotropic cylinder. So, it was demonstrated that for a cluster of N cylinders the coefficient of the lower order term in the series expansion of element $(T_{\text{eff}})_{00}$ is

$$(\hat{T}_{\text{eff}})_{00} \equiv \lim_{k\to 0} \frac{(T_{\text{eff}})_{00}}{k^2} = \sum_{\alpha} (\hat{T}_{\alpha})_{00}, \tag{41}$$

where $(\hat{T}_{\alpha})_{00}$ is the corresponding coefficient of the α-cylinder in the cluster. For the case of equal cylinders, the matrix elements $(\hat{T}_{\alpha})_{00}$ are all identical and

$$(\hat{T}_{\text{eff}})_{00} = \mathrm{i}N \frac{\pi R_{\text{a}}^2}{4} \left[\frac{B_b}{B_a} - 1 \right], \tag{42}$$

where R_a and B_a are the radius and bulk modulus of cylinders, respectively.

Here, we are dealing with a cluster based on anisotropic lattices and, therefore, it is expected that such cluster behaves (in the regime of large wavelengths) as an effective anisotropic fluid-like cylinder with some effective radius R_{eff} that also has to be determined.

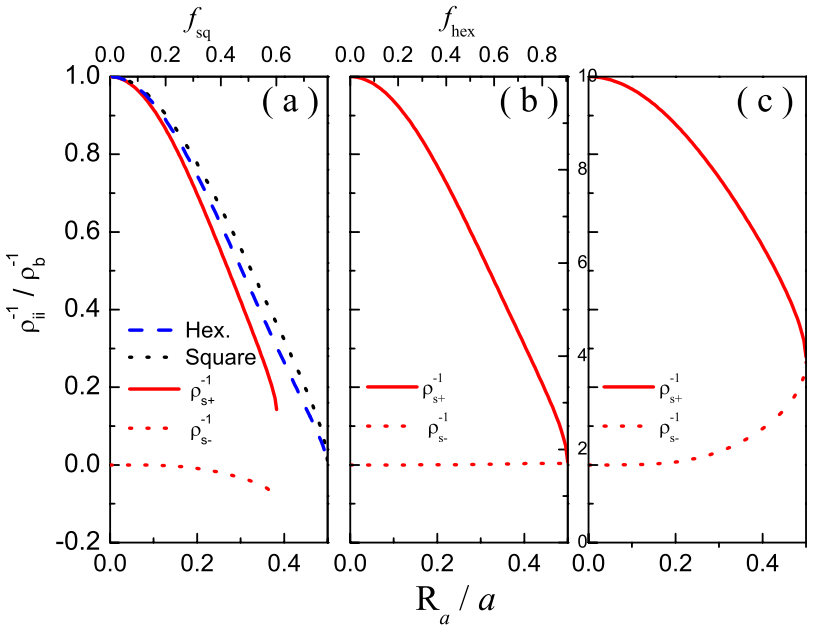

Figure 7. Reciprocal of the effective density tensor as a function of the radius of cylinders in reduced units (R_a/a) for three different anisotropic lattices: (a) $a_2 = a_1$, $\phi = 45°$; (b) $a_2 = a_1$, $\phi = 75°$; and (c) $a_2 = 2a_1$, $\phi = 75°$. Results for the 2D isotropic lattices (hexagonal and square) are also shown in (a) comparison.

Appendix A shows that the coefficient $\hat{T}_{00}$ of an anisotropic fluid-like cylinder is equal to that of an isotropic fluid-like cylinder. Therefore, following the method developed in [12]

$$\mathrm{i}\frac{\pi R_{\mathrm{eff}}^2}{4}\left[\frac{B_b}{B_{\mathrm{eff}}} - 1\right] = \mathrm{i}N\frac{\pi R_a^2}{4}\left[\frac{B_b}{B_a} - 1\right], \tag{43}$$

where the left side in this expression is the coefficient $(\hat{T}_{\mathrm{eff}})_{00}$ of the homogenized cluster with effective bulk modulus B_{eff} and R_{eff} being its effective radius. R_{eff} can be obtained by a simple approach: it is assumed that the fraction of volume occupied by the cylinders is equal to the filling fraction of the underlying lattice, f, that is

$$\frac{N(\pi R_a^2)}{\pi R_{\mathrm{eff}}^2} = f \tag{44}$$

Now, with the value of R_{eff} it is possible to obtain B_{eff} from (43):

$$\frac{1}{B_{\mathrm{eff}}} = \frac{f}{B_a} + \frac{1-f}{B_b}. \tag{45}$$

This is the standard averaging of bulk moduli that has been previously shown to be valid for isotropic 2D lattices of composites made of elastic cylinders [14, 15].

With B_{eff} and the velocity tensor, we are ready to determine the reciprocal density tensor and, then, to fully characterize the anisotropic medium.

4.3. Effective mass density

With the expressions derived above, the reciprocal density tensor are derived from $\rho_{\text{eff}}^{-1}(\theta) = c_{\text{eff}}^2(\theta)/B_{\text{eff}}$:

$$\rho_{s+}^{-1} = \frac{|\Delta|^2 - |\Gamma|^2 - f^2\eta^2}{(\Delta + f\eta)(\Delta^* + f\eta) - |\Gamma|^2}, \tag{46a}$$

$$\rho_{s-}^{-1} = -\frac{2f\eta|\Gamma|\cos\Phi_\Gamma}{(\Delta + f\eta)(\Delta^* + f\eta) - |\Gamma|^2}, \tag{46b}$$

$$\rho_{a+}^{-1} = \frac{2f\eta|\Gamma|\sin\Phi_\Gamma}{(\Delta + f\eta)(\Delta^* + f\eta) - |\Gamma|^2}. \tag{46c}$$

It is important to note that the reciprocal density tensor (and the effective density) does not depend on the bulk modulus of background and cylinder. In other words, the effective density only depends on the lattice structure, its filling fraction and the density of cylinders relative to the background. The elastic nature of cylinders will be only present in the effective density for high filling fractions, where the higher orders of the T matrix will be present in both the Δ and Γ factors.

Figure 7 plots the behavior of the reciprocal density tensor as a function of the cylinder radius (in units of a) for three different anisotropic lattices. For the sake of comparison, the results for the isotropic lattices, hexagonal and square, are depicted in figure 7(a). Note that the stronger anisotropy is achieved for the case (c), which corresponds to the lattice having the larger value of anisotropy strength A_Γ (see figure 3).

4.3.1. Isotropic lattices. For the case of isotropic lattices ($\Gamma = 0$) the effective velocity (39) can be also cast as:

$$\bar{c}_{\text{eff}}^2 = \frac{1}{\rho_{\text{eff}}} \cdot \frac{B_a}{fB_b + (1-f)B_a}, \tag{47}$$

in which:

$$\rho_{\text{eff}} = \frac{\rho_a(\Delta + f) + \rho_b(\Delta - f)}{\rho_a(\Delta - f) + \rho_b(\Delta + f)}\rho_b. \tag{48}$$

The second factor in the right hand side of (47) is the effective bulk modulus B_{eff} given in (45). It can be demonstrated that for low enough f (i.e. $\Delta = 1$) the expression (48) reduces to that obtained by Berryman [17] for the dimensionality parameter $d = 2$ (see also equation (2) in [10]).

5. Effective parameters for lattices of elastic cylinders

When the ratio between acoustic impedances of cylinders and background Z_a/Z_b is not large enough the condition of rigid cylinders (i.e. $\rho = \infty$) is not valid and the sound propagation inside the cylinders has to be taken into account. This is the usual case when working with solid cylinders embedded in water. Therefore, the full elastic properties of cylinders must be considered in the corresponding T matrix. As a consequence, the effective parameters of metamaterials based on solid cylinders embedded in a fluid, like water, present a rich variety of behavior depending of the ratio Z_a/Z_b, the lattice topology and the fraction of

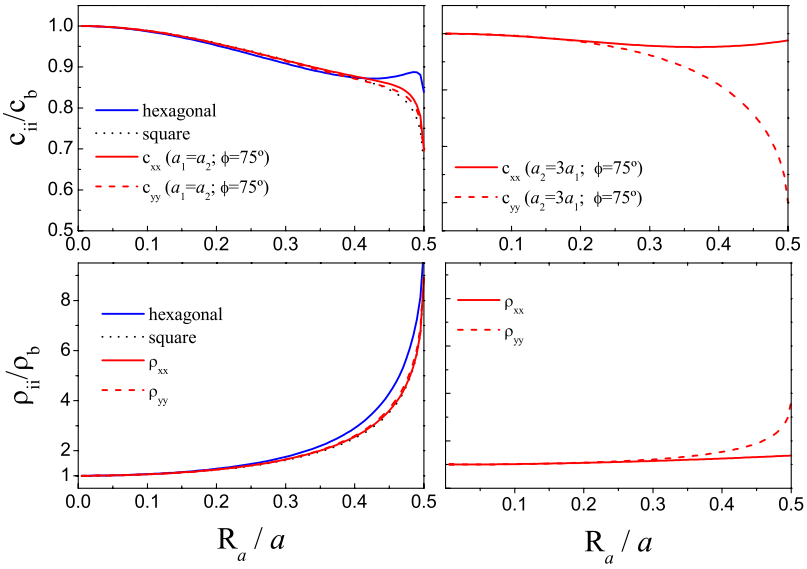

Figure 8. Effective parameters for 2D arrays of lead (Pb) cylinders embedded in water for the two isotropic lattices (hexagonal and square) and two different anisotropic lattices.

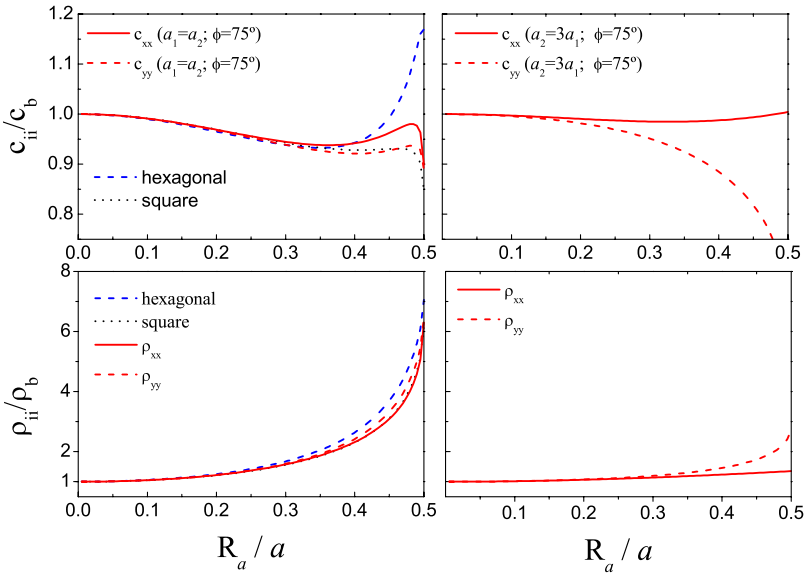

Figure 9. Effective parameters for 2D arrays of iron (Fe) cylinders embedded in water for the two isotropic lattices (hexagonal and square) and two different anisotropic lattices.

volume (f) occupied by the cylinders in the corresponding lattice. As an example of typical behaviors encountered, figures 8–10 represent the cases of cylinders made of lead (Pb), iron (Fe) and aluminium (Al), respectively, embedded in water. The data parameters employed in the numerical simulations are reported in table 2. Results are shown for the two 2D isotropic

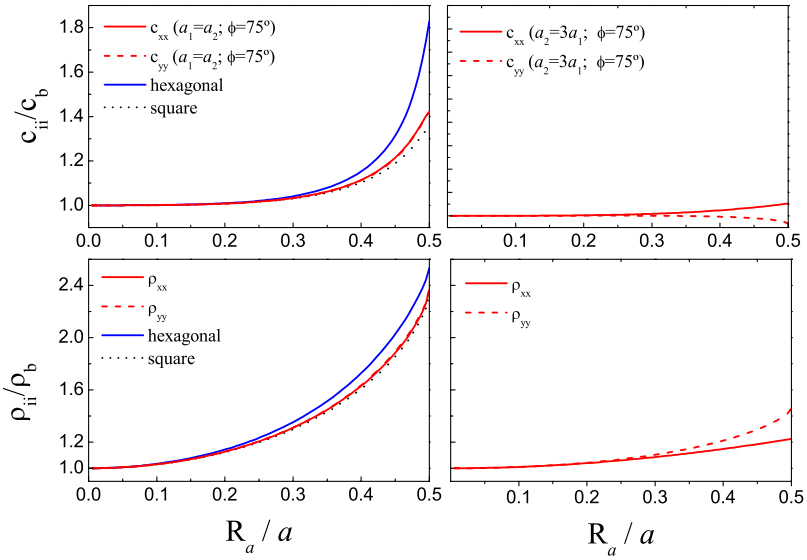

Figure 10. Effective parameters for 2D arrays of aluminium (Al) cylinders embedded in water for the two isotropic lattices (hexagonal and square) and two different anisotropic lattices.

Table 2. Elastic parameters of materials studied in this work. The density, ρ_a, and the fluidlike velocity, $c_a \equiv \sqrt{c_\ell^2 - c_\mathrm{t}^2}$ (where c_ℓ and c_t are the longitudinal and transversal velocities, respectively) are normalized to those of water ($\rho_\mathrm{b} = 1\,\mathrm{g\,cm^{-3}}$ and $c_\mathrm{b} = 1.45\,\mathrm{cm\,sec^{-1}}$).

	$\overline{\rho}_a$	$\overline{c}_\ell$	$\overline{c}_\mathrm{t}$	$\overline{c}_a$	$\overline{Z}_a$
Pb	11.40	1.37	0.47	1.28	13.44
Fe	7.86	3.95	2.15	3.31	26.5
Al	2.70	4.24	2.09	3.69	13.91

lattices (square and hexagonal) and two anisotropic lattices. As anisotropic lattice we have studied one ($a_1 = a_2$ and $\phi = 75^\circ$) characterized by a very small anisotropic strength parameter ($A_\Gamma = 0.001$) and another ($a_1 = 3a_2$ and $\phi = 75^\circ$) in which this parameter is more than one order of magnitude larger ($A_\Gamma = 0.042$).

Results for the slightly anisotropic lattice ($A_\Gamma = 0.001$) in the left panels of figures 8–10 show that the values of their effective parameters are in between of those calculated for the hexagonal ($\phi = 60^\circ$) and square ($\phi = 90^\circ$) lattices and the difference between diagonal elements is very small. Results for the stronger anisotropic lattice are depicted in the right panels of the same figures. They show that diagonal elements show appreciable differences that increase with cylinder radius and should be observable in acoustic experiments. Also note that the difference between diagonal elements decreases with decreasing density. Therefore, we can conclude that in order to observe strong anisotropic effects in lattices of solid cylinders embedded in a fluid, we have to select a lattice with a large value of A_Γ made of cylinders with a density as large as possible in comparison with that of the fluid background.

6. Summary

To summarize, this work has introduced a method to create acoustic metamaterials having anisotropic dynamical mass density and sound speed. The method is based on the properties of SC in the homogenization limit. It was shown that 2D arrays of cylinders ordered in lattices with symmetries other than the square and hexagonal symmetry behave in the range of large wavelengths as effective acoustic metamaterials having acoustic parameters (mass density and velocity) that are anisotropic. Analytical results for both parameters have been rigorously derived and numerical calculations have been presented for relevant examples like the case of rigid cylinders in air and some elastic cylinders embedded in water. This work should be considered as a demonstration that anisotropic fluidlike acoustic materials can be physically realizable. The possible applications of these structures strongly depend on the properties of wave propagation through them and will be the topic of our next work. However, we can foresee that these structures could be the basis of designing the class of anisotropic materials needed to demonstrate the acoustic cloaking recently predicted by Cummer and Schurig [18].

Acknowledgments

We are grateful for the financial support provided by the Spanish Ministry of Science and Education (MEC) under projects TEC2005-03545 and TEC2007-67239, and by Generalitat Valenciana (project ACOMP07-204). DT acknowledges a PhD grant also supported by the MEC.

Appendix A. $\hat{T}_{00}$ for a homogeneous anisotropic cylinder

The starting point to obtain $\hat{T}_{00}$, which represents the coefficient of the lower order term in the series expansion of element T_{00} of an anisotropic cylinder, is the T matrix of the given cylinder. We have obtained the analytical expression for the T matrix of a homogeneous anisotropic cylinder that, here, will be introduced without details. The derivation of the T matrix is out of the scope of the present work and will be reported in a more specialized journal. However, the readers are directed to the article by Monzon and Damaskos [29], where a procedure analogous to that employed by us is applied to the case of a homogeneous anisotropic dielectric rod.

Let us consider an anisotropic cylinder of radius R_0 embedded in a nonviscous liquid or gas. The speed of sound inside the cylinder is given by the tensor $\overline{c}_{ij}$, and its bulk modulus $\overline{B}_0$ (a scalar) related with the anisotropic density by the Wood's law (8) as $\overline{c}_{ij} = \overline{B}_0(\overline{\rho}_{ij})^{-1}$. All the magnitudes associated to the cylinder are normalized to the corresponding ones of the embedding medium. The T matrix for this cylinder, $\mathcal{T}$, can be easily obtained by studying the scattering of a plane wave of wavenumber k impinging the cylinder. After applying boundary conditions on the cylinder's surface, it is found that

$$\mathcal{T}\mathcal{H} = -\mathcal{J} \tag{A.1}$$

or equivalently

$$\mathcal{T} = -\mathcal{J}\mathcal{H}^{-1}, \tag{A.2}$$

where $\mathcal{J}$ and $\mathcal{H}$ are matrices whose matrix elements are:

$$J_{sq} = \frac{\mathrm{i}\pi R_0}{2}\left[k J_q'(kR_0)\,\Xi_{sq}^{(1)} - J_q(kR_0)\,\Xi_{sq}^{(2)}\right], \tag{A.3}$$

$$H_{sq} = \frac{\mathrm{i}\pi R_0}{2}\left[kH_q'(kR_0)\Xi_{sq}^{(1)} - H_q(kR_0)\Xi_{sq}^{(2)}\right], \tag{A.4}$$

where $J_q'(\cdot)$ and $H_q'(\cdot)$ are the derivatives of Bessel and Hankel function of order q with respect to its argument and

$$\Xi_{sq}^{(1)} = \frac{\mathrm{i}^{-s}}{4\pi^2}\int_0^{2\pi}\int_0^{2\pi} \mathrm{e}^{\mathrm{i}\frac{kR_0}{c(\alpha)}\cos(\alpha-\theta)}\mathrm{e}^{\mathrm{i}s\alpha}\mathrm{e}^{-\mathrm{i}q\theta}\,\mathrm{d}\alpha\,\mathrm{d}\theta, \tag{A.5}$$

$$\Xi_{sq}^{(2)} = \frac{\mathrm{i}^{-s}}{4\pi^2}\int_0^{2\pi}\int_0^{2\pi} \rho^{-1}:\nabla\big|_{r=R_0}\,\mathrm{e}^{\mathrm{i}\frac{kr}{c(\alpha)}\cos(\alpha-\theta)}\mathrm{e}^{\mathrm{i}s\alpha}\mathrm{e}^{-\mathrm{i}q\theta}\,\mathrm{d}\alpha\,\mathrm{d}\theta. \tag{A.6}$$

The expression $\rho^{-1}:\nabla$ defines the following operator (in polar coordinates):

$$\rho^{-1}:\nabla \equiv \rho_{rr}^{-1}\frac{\partial}{\partial r} + \frac{\rho_{r\theta}^{-1}}{r}\frac{\partial}{\partial\theta}. \tag{A.7}$$

The first diagonal element T_{00} can be obtained from (A.1), which in terms of matrix elements is

$$\sum_r T_{sr}H_{rq} = -J_{sq}. \tag{A.8}$$

When both q and s are equal to zero, this expression reduces to

$$T_{00}H_{00} = -J_{00} - \sum_{r\neq 0} T_{0r}H_{r0}. \tag{A.9}$$

It can be demonstrated that the second term in the right-hand side is of higher order in k than J_{00}.

Now, in the limit of $k\to 0$, the k's dependent exponential in $\Xi_{sq}^{(1)}$ and $\Xi_{sq}^{(2)}$ can be expanded in powers of k as follows:

$$\mathrm{e}^{\mathrm{i}\frac{kR_0}{c(\alpha)}\cos(\alpha-\theta)} \approx 1 + \mathrm{i}\frac{kR_0}{c(\alpha)}\cos(\alpha-\theta) - \frac{k^2R_0^2}{2c^2(\alpha)}\cos^2(\alpha-\theta). \tag{A.10}$$

By including this expansion in $\Xi_{00}^{(1)}$ and $\Xi_{00}^{(2)}$ and after integrating in θ it is found that

$$\Xi_{00}^{(1)} \approx 1 + \mathcal{O}(k), \tag{A.11}$$

$$\Xi_{00}^{(2)} \approx -\frac{R_0}{2\overline{B}_0}k^2 + \mathcal{O}(k^3). \tag{A.12}$$

Therefore

$$J_{00} \approx \mathrm{i}\frac{\pi R_0^2}{4}\left[\frac{1}{\overline{B}_0} - 1\right]k^2 + \mathcal{O}(k^4), \tag{A.13}$$

$$H_{00} \approx -1 + \mathcal{O}(k\ln k), \tag{A.14}$$

which can be used to obtain T_{00} as $T_{00} = -J_{00}/H_{00}$.

Finally, the coefficient of lower order in k is easily determined

$$\hat{T}_{00} = \lim_{k\to 0} \frac{T_{00}}{k^2} = \frac{\mathrm{i}\pi R_0^2}{4}\left[\frac{1}{\overline{B}_0} - 1\right]. \tag{A.15}$$

Note that this expression is the same as that obtained for the case of a homogeneous isotropic cylinder [12].

Appendix B. Asymptotic expression of the M matrix in the low frequency limit

This appendix is devoted to obtain the asymptotic form of the secular equation associated to the M matrix whose elements are given in (23). The determinant of the $(2Q_{\max}+1)\times(2Q_{\max}+1)$ final matrix will be reduced computed from the determinant of a 3×3 matrix. Let's do it by computing first the diagonal elements.

B.1. Diagonal terms: $q = s$

To determine the asymptotic form of terms

$$\hat{M}_{qq} = 1 - \mathrm{i}\hat{T}_{\mathrm{q}} \lim_{k\to 0} S_0^Y k^{2|q|+2\delta_{q0}} \tag{B.1}$$

the asymptotic form of S_0 must be computed. We know that

$$S_0^Y k^{2|q|+2\delta_{q0}} = -\frac{4}{V_{\mathrm{d}}}\left[\frac{k}{J_1(kR_{\min})}\frac{J_1(KR_{\min})}{K(K^2-k^2)} + \frac{k}{J_1(kR_{\min})}\sum_{h\neq 0}\frac{J_1(G_h R_{\min})}{G_h^3}\right] k^{2|q|+2\delta_{q0}}, \tag{B.2}$$

where K is a Bloch wavenumber ($\mathbf{K} = K\cos\theta\hat{\mathbf{x}} + K\sin\theta\hat{\mathbf{y}}$).

In this expression only the first term will contribute to the matrix, so that

$$S_0^Y k^{2|q|+2\delta_{q0}} = -\frac{4}{V_{\mathrm{d}}}\frac{k^{2|q|+2\delta_{q0}}}{K^2-k^2}. \tag{B.3}$$

Since the speed of sound is defined by $c = \lim_{k\to 0}(k/K)$ (to simplify the notation in this appendix) only the $q = 0, \pm 1$ terms will contribute to the matrix, then

$$\hat{M}_{00} = 1 - f\left[\frac{1}{\overline{B}_a} - 1\right]\frac{\overline{c}^2}{1-\overline{c}^2}, \tag{B.4}$$

$$\hat{M}_{11} = 1 - f\left[\frac{\overline{\rho}_a - 1}{\overline{\rho}_a + 1}\right]\frac{\overline{c}^2}{1-\overline{c}^2} = \hat{M}_{-1-1}, \tag{B.5}$$

$$\hat{M}_{qq} = 1; \quad \forall |q| \geqslant 2, \tag{B.6}$$

where $\overline{B}_a = B_a/B_{\mathrm{b}}$, $\overline{\rho}_a = \rho_a/\rho_{\mathrm{b}}$ and $\overline{c} = c_a/c_{\mathrm{b}}$.

B.2. Matrix elements with $s > q$

To calculate these nondiagonal elements we split the lattice sum into two separate terms:

$$S^{Y}_{s-q} k^{|q|+|s|+\delta_{q0}+\delta_{s0}} = S^{c}_{s-q} + S^{G}_{s-q}, \tag{B.7}$$

where

$$S^{c}_{s-q} = -\frac{4}{V_{\mathrm{d}}} \mathrm{i}^{s-q} \frac{k}{J_{s-q+1}(kR_{\min})} \frac{J_{s-q+1}(KR_{\min})}{K(K^2-k^2)} \mathrm{e}^{\mathrm{i}(s-q)\theta_0} k^{|q|+|s|+\delta_{q0}+\delta_{s0}}, \tag{B.8}$$

$$S^{G}_{s-q} = -\frac{4}{V_{\mathrm{d}}} \mathrm{i}^{s-q} \frac{k}{J_{s-q+1}(kR_{\min})} \sum_{h\neq 0} \frac{J_{s-q+1}(G_h R_{\min})}{G_h^3} \mathrm{e}^{\mathrm{i}(s-q)\theta_h} k^{|q|+|s|+\delta_{q0}+\delta_{s0}}. \tag{B.9}$$

For $k \to 0$ we use the asymptotic expressions of Bessel functions to get

$$S^{c}_{s-q} = -\frac{4}{V_{\mathrm{d}}} \mathrm{i}^{s-q} \frac{k^{|q|+|s|+\delta_{q0}+\delta_{s0}}}{c^{s-q}} \frac{1}{K^2-k^2} \mathrm{e}^{\mathrm{i}(s-q)\theta_0}, \tag{B.10}$$

$$S^{G}_{s-q} = -\frac{4}{V_{\mathrm{d}}} \mathrm{i}^{s-q} 2^{s-q+1}(s-q+1)! \frac{k^{|q|+|s|+\delta_{q0}+\delta_{s0}}}{k^{s-q} R_{\min}^{s-q+1}} \sum_{h\neq 0} \frac{J_{s-q+1}(G_h R_{\min})}{G_h^3} \mathrm{e}^{\mathrm{i}(s-q)\theta_h}. \tag{B.11}$$

Only those terms independent of k will survive to the limit. So, the condition to have the factor $S^{\upsilon}_{s-q} \neq f(k)$ is

$$|q| + |s| + \delta_{q0} + \delta_{s0} = 2 \to (q, s) = (0, 1), (-1, 0), (-1, 1). \tag{B.12}$$

In the same manner, the factor $S^{G}_{s-q} \neq f(k)$ if

$$|q| + |s| + \delta_{q0} + \delta_{s0} - s + q = 0 \to s > 0, \quad q < 0. \tag{B.13}$$

Therefore, the contributions to the matrix are

$$S^{c}_{s-q} = -\frac{4}{V_{\mathrm{d}}} \mathrm{i}^{|s|+|q|} \frac{c^2}{c^{|s|+|q|}} \frac{1}{1-c^2} \mathrm{e}^{\mathrm{i}(|s|+|q|)\theta}, \quad \text{for } |qs| \leqslant 1, \quad s > q, \tag{B.14}$$

$$S^{G}_{s-q} = -\frac{4}{V_{\mathrm{d}} R_{\min}^{|s|+|q|+1}} \mathrm{i}^{|s|+|q|} 2^{|s|+|q|+1}(|s|+|q|+1)! \sum_{h\neq 0} \frac{J_{|s|+|q|+1}(G_h R_{\min})}{G_h^3} \mathrm{e}^{\mathrm{i}(|s|+|q|)\theta_h}, \quad s > 0, \quad q < 0 \tag{B.15}$$

and

$$\hat{M}_{qs} = \delta_{qs} - \mathrm{i}\hat{T}_q S^{Y}_{s-q}. \tag{B.16}$$

B.3. Matrix elements with $q > s$

In this case, we know that $S^{Y}_{s-q} = S^{Y}_{-(q-s)} = S^{Y^*}_{(q-s)}$, and, by remembering that $\mathrm{i}\hat{T}_q$ is a real number, we have

$$\hat{M}_{qs} = \delta_{qs} - \mathrm{i}\hat{T}_q S^{Y}_{s-q} = \delta_{qs} - \mathrm{i}\hat{T}_q (S^{Y}_{q-s})^* = \delta_{qs} - (\mathrm{i}\hat{T}_q S^{Y}_{q-s})^*. \tag{B.17}$$

B.4. Final expression of $\hat{M}$

By defining $Q \equiv 2(Q_{\max} - 1)$, we can reorder the $\hat{M}$ matrix as

$$\hat{M} = \begin{pmatrix} A_{3\times 3} & B_{3\times Q} \\ C_{Q\times 3} & D_{Q\times Q} \end{pmatrix}, \tag{B.18}$$

being

$$A = \begin{pmatrix} 1 - \eta\dfrac{\overline{c}^2}{1-c^2} f & \mathrm{i}\eta\dfrac{\overline{c}}{1-\overline{c}^2} f \mathrm{e}^{-\mathrm{i}\theta} & \eta\dfrac{1}{1-\overline{c}^2} f \mathrm{e}^{-2\mathrm{i}\theta} + \Gamma^{(0)} \\ -\mathrm{i}\zeta\dfrac{\overline{c}}{1-\overline{c}^2} f \mathrm{e}^{\mathrm{i}\theta} & 1 - \zeta\dfrac{\overline{c}^2}{1-\overline{c}^2} f & \mathrm{i}\zeta\dfrac{\overline{c}}{1-\overline{c}^2} f \mathrm{e}^{-\mathrm{i}\theta} \\ \eta\dfrac{1}{1-\overline{c}^2} f \mathrm{e}^{2\mathrm{i}\theta} + \Gamma^{(0)*} & -\mathrm{i}\eta\dfrac{\overline{c}}{1-\overline{c}^2} f \mathrm{e}^{\mathrm{i}\theta} & 1 - \eta\dfrac{\overline{c}^2}{1-\overline{c}^2} f \end{pmatrix}, \tag{B.19}$$

where $\eta = (\rho_a - \rho_\mathrm{b})/(\rho_a + \rho_\mathrm{b})$ and $\zeta = B_\mathrm{b}/B_a - 1$, B_a (ρ_a) and B_b (ρ_b) being the elastic moduli (densities) of cylinders and background, respectively. Finally, θ is the angle of Bloch wavevector with x-axis and $\Gamma^{(0)}$ is the anisotropy factor defined as

$$\Gamma^{(0)} = 48\eta f \sum_{h\neq 0} \frac{J_3(G_h R_{\min})}{G_h^3 R_{\min}^3} \mathrm{e}^{-2\mathrm{i}\theta_h}. \tag{B.20}$$

The matrix D has the form

$$D = \begin{pmatrix} I & D_{q>s} \\ D_{q<s} & I \end{pmatrix}, \tag{B.21}$$

$$D_{q<s}|_{qs} \equiv D_{-qs} = -8\mathrm{i}^{s+q} 2^{s-q} \frac{(s+q+1)!}{q!(q-1)!} \frac{R_\mathrm{a}^{2(q-1)}}{R_{\min}^{s+q+1}} f \eta^\mathrm{e} \sum_{h\neq 0} \frac{J_{s+q+1}(G_h R_{\min})}{G_h^3} \mathrm{e}^{\mathrm{i}(s+q)\theta_h}, \tag{B.22}$$

$$D_{q>s}|_{qs} \equiv D_{q-s} = (D_{-qs})^*, \tag{B.23}$$

where $\eta^\mathrm{e} = (\rho_a - \rho_\mathrm{b})/(\rho_a + \rho_\mathrm{b})$ for fluid like cylinders and $\eta^\mathrm{e} = 1$ for full elastic cylinders.

For the B and C matrices we have

$$B = \begin{pmatrix} O & B_{1-s} \\ O & O \\ B_{-1s} & O \end{pmatrix}, \tag{B.24}$$

$$B_{-1s} = 4\mathrm{i}^{s+1} 2^s (s+2)! \frac{f\eta}{R_{\min}^{s+2}} \sum_{h\neq 0} \frac{J_{s+2}(G_h R_{\min})}{G_h^3} \mathrm{e}^{\mathrm{i}(s+1)\theta_h}, \tag{B.25}$$

$$B_{1-s} = (B_{-1s})^*, \tag{B.26}$$

$$C = \begin{pmatrix} O & O & C_{q-1} \\ C_{-q1} & O & O \end{pmatrix}, \tag{B.27}$$

$$C_{-q1} = -16\mathrm{i}^{q+1} 2^{-q} \frac{(q+2)!}{q!(q-1)!} \frac{R_a^{2(q-1)}}{R_{\min}^{q+2}} f \eta^e \sum_{h\neq 0} \frac{J_{q+2}(G_h R_{\min})}{G_h^3} \mathrm{e}^{\mathrm{i}(1+|q|)\theta_h}, \tag{B.28}$$

$$C_{q-1} = (C_{-q1})^*. \tag{B.29}$$

B.5. The 3×3 *secular equation*

The secular equation (29) is impossible to solve analytically since it depends on the number of angular momenta employed to ensure convergence. Instead, we should look for a more suitable secular equation so that its analytical solution will not depend on such convergence condition. To achieve this goal let us define the matrix X:

$$X \equiv \begin{pmatrix} I_{3\times 3} & O_{3\times Q} \\ -D^{-1}C|_{Q\times 3} & D^{-1}_{Q\times Q} \end{pmatrix}. \tag{B.30}$$

Note that $\det X = \det D^{-1}$. Now, by means of the product MX,

$$MX = \begin{pmatrix} A - BD^{-1}C|_{3\times 3} & BD^{-1}|_{3\times Q} \\ O_{Q\times 3} & I_{Q\times Q} \end{pmatrix}, \tag{B.31}$$

we arrive at the following relationships:

$$\det(MX) = \det M \det X = \det M \det D^{-1},$$

$$\det(MX) = \det(A - BD^{-1}C).$$

Let us assume that $\det D \neq 0$, the condition over the M matrix of dimension $2(Q_{\max+1}) \times 2(Q_{\max+1})$, becomes a condition over the matrix $A - BD^{-1}C$ of dimension 3×3. In other words, the secular equation $\det \hat{M} = 0$ is reduced to $\det(A - BD^{-1}C) = 0$, which can be solved analytically.

The matrix elements of $BD^{-1}C$ are

$$BD^{-1}C\big|_{k\ell} = \sum_s \sum_q B_{ks} D^{-1}_{sq} C_{q\ell}. \tag{B.32}$$

By using the definitions of matrices B and C it is straightforward to verify that

$$BD^{-1}C\big|_{0\ell} = BD^{-1}C\big|_{k0} = 0, \qquad \forall k, \ell. \tag{B.33}$$

The expression for the diagonal terms are:

$$BD^{-1}C\big|_{11} = \sum_s \sum_q B_{1s} D^{-1}_{sq} C_{q1} = \sum_{s>1} \sum_{q>1} B_{1-s} D^{-1}_{-s-q} C_{-q1},$$

$$BD^{-1}C\big|_{-1-1} = \sum_s \sum_q B_{-1s} D^{-1}_{sq} C_{q-1} = \sum_{s>1} \sum_{q>1} B_{-1s} D^{-1}_{sq} C_{q-1},$$

$$= \sum_{s>1} \sum_{q>1} B^*_{1-s} D^{-1}_{sq} C^*_{-q1}.$$

From the definition of matrix D^{-1} we have that

$$\sum_s D_{\ell s} D^{-1}_{sq} = \sum_{s>0} D_{-\ell s} D^{-1}_{sq} = \delta_{\ell q}$$

$$\sum_s D_{\ell s} D^{-1}_{-s-q} = \sum_{s>0} D_{\ell -s} D^{-1}_{-s-q} = \delta_{\ell -q} = \sum_{s>0} D^*_{-\ell s} D^{-1}_{-s-q} = \delta_{-\ell -q} = \delta_{\ell q}.$$

So that $D_{sq}^{-1} = D_{-s-q}^{-1^*}$ and we conclude that

$$BD^{-1}C\big|_{-1-1} = BD^{-1}C\big|_{11}^{*}. \tag{B.34}$$

Following the same procedure we obtain:

$$\begin{aligned} BD^{-1}C\big|_{-11} &= \sum_{s}\sum_{q} B_{-1s}D_{sq}^{-1}C_{q1} = \sum_{s>1}\sum_{q>1} B_{-1s}D_{s-q}^{-1}C_{-q1}, \\ BD^{-1}C\big|_{1-1} &= \sum_{s}\sum_{q} B_{1s}D_{sq}^{-1}C_{q-1} = \sum_{s>1}\sum_{q>1} B_{1-s}D_{-sq}^{-1}C_{q-1} \\ &= \sum_{s>1}\sum_{q>1} B_{-1s}^{*}D_{-sq}^{-1}C_{-q1}^{*} \end{aligned}$$

and

$$\begin{aligned} \sum_{s} D_{-\ell s}D_{s-q}^{-1} &= \sum_{s>0} D_{-\ell s}D_{s-q}^{-1} = \delta_{-\ell-q} = \delta_{\ell q}, \\ \sum_{s} D_{ls}D_{-sq}^{-1} &= \sum_{s>0} D_{l-s}D_{-sq}^{-1} = \delta_{lq} = \sum_{s>0} D_{-ls}^{*}D_{-sq}^{-1} = \delta_{-\ell-q} = \delta_{\ell q}. \end{aligned}$$

In a similar manner $D_{-sq}^{-1} = D_{s-q}^{-1^*}$ and

$$BD^{-1}C\big|_{-11} = BD^{-1}C\big|_{1-1}^{*}. \tag{B.35}$$

In conclusion, the matrix $BD^{-1}C$ takes the form

$$BD^{-1}C = \begin{pmatrix} \Delta' & 0 & \Gamma' \\ 0 & 0 & 0 \\ \Gamma'^{*} & 0 & \Delta'^{*} \end{pmatrix} \tag{B.36}$$

and therefore

$$A - BD^{-1}C = \begin{pmatrix} 1-\Delta' - f\eta\dfrac{\overline{c}^2}{1-\overline{c}^2} & \mathrm{i}\eta\dfrac{\overline{c}}{1-c^2}f\mathrm{e}^{-\mathrm{i}\theta} & \eta\dfrac{1}{1-c^2}f\mathrm{e}^{-2\mathrm{i}\theta} + \Gamma^{(0)} - \Gamma' \\ -\mathrm{i}\zeta\dfrac{\overline{c}}{1-\overline{c}^2}f\mathrm{e}^{\mathrm{i}\theta} & 1-\zeta\dfrac{\overline{c}^2}{1-\overline{c}^2}f & \mathrm{i}\zeta\dfrac{\overline{c}}{1-\overline{c}^2}f\mathrm{e}^{-\mathrm{i}\theta} \\ \eta\dfrac{1}{1-\overline{c}^2}f\mathrm{e}^{-2\mathrm{i}\theta} + \Gamma^{(0)*} - \Gamma'^{*} & -\mathrm{i}\eta\dfrac{\overline{c}}{1-\overline{c}^2}f\mathrm{e}^{\mathrm{i}\theta} & 1-\Delta'^{*} - \eta\dfrac{\overline{c}^2}{1-\overline{c}^2}f \end{pmatrix}. \tag{B.37}$$

In function of the new variables defined as:

$$\Delta \equiv 1 - \Delta', \tag{B.38}$$

$$\Gamma \equiv \Gamma^{(0)} - \Gamma' = |\Gamma|\,\mathrm{e}^{\mathrm{i}\Phi_\Gamma} \tag{B.39}$$

the 3×3 secular equation takes the following final expression after straightforward manipulations:

$$\det\left|A-BD^{-1}C\right| = \frac{1}{(1-\bar{c}^2)^3}\det\begin{vmatrix} (1-\bar{c}^2)\Delta-\eta\bar{c}^2 f & \mathrm{i}\eta\bar{c}\,f & \eta f+(1-\bar{c}^2)\Gamma \mathrm{e}^{2\mathrm{i}\theta} \\ -\mathrm{i}\zeta\bar{c}\,f & (1-\bar{c}^2)-\zeta\bar{c}^2 f & \mathrm{i}\zeta\bar{c}\,f \\ \eta f+(1-\bar{c}^2)\Gamma^* \mathrm{e}^{-\mathrm{i}2\theta} & -\mathrm{i}\eta f\bar{c} & (1-\bar{c}^2)\Delta^*-\eta\bar{c}^2 f \end{vmatrix}. \tag{B.40}$$

References

[1] Sánchez-Pérez J V, Caballero D, Martinez-Sala R, Rubio C, Sánchez-Dehesa J, Meseguer F and Gálvez F 1998 Sound attenuation by a two-dimensional array of rigid cylinders *Phys. Rev. Lett.* **80** 5325

[2] Cervera F, Sanchis L, Sánchez-Pérez J V, Martínez-Sala R, Rubio C, Meseguer F, López C, Caballero D and Sánchez-Dehesa J 2002 Refractive acoustic devices for airborne sound *Phys. Rev. Lett.* **88** 023902

[3] Krokhin A A, Arriaga J and Gumen L N 2003 Speed of sound in periodic elastic composites *Phys. Rev. Lett.* **91** 264302

[4] Sanchis L, Håkansson A, Cervera F and Sánchez-Dehesa J 2003 Acoustic interferometers based on two-dimensional arrays of rigid cylinders in air *Phys. Rev.* B **67** 035422

[5] Gupta B C and Ye Z 2003 Theoretical analysis of the focusing of acoustic waves by two-dimensional sonic crystals *Phys. Rev.* E **67** 036603

[6] Garcia N, Nieto-Vesperinas M, Ponizovskaya E V and Torres M 2003 Theory of tailoring sonic devices: diffraction dominates over refraction *Phys. Rev.* E **67** 046606

[7] Li J and Chan C T 2004 Double-negative acoustic metamaterial *Phys. Rev.* E **70** 055602

[8] Håkansson A, Sánchez-Dehesa J, Cervera F, Meseguer M, Sanchis L and Llinares J 2005 Comment on theory of tailoring sonic devices: diffraction dominates over refraction *Phys. Rev.* E **71** 018601

[9] Hou Z, Wu F, Fu X and Liu Y 2005 Effective elastic parameters of two-dimensional elastic crystals *Phys. Rev.* E **71** 037604

[10] Mei J, Liu Z, Wen W and Sheng P 2006 Effective mass density of fluid-solid composites *Phys. Rev. Lett.* **96** 024301

[11] Torrent D, Håkansson A, Cervera F and Sànchez-Dehesa J 2006 Homogenization of two-dimensional clusters of rigid rods in air *Phys. Rev. Lett.* **96** 204302

[12] Torrent D and Sánchez-Dehesa J 2006 Effective parameters of clusters of cylinders embedded in a nonviscous fluid or gas *Phys. Rev.* B **74** 224305

[13] Li S, George T F, Chen L S, Sun X and Kuo C H 2006 Disorder effect on the focus image of sonic crystals in air *Phys. Rev.* E **73** 056615

[14] Torrent D and Sánchez-Dehesa J 2007 Evidence of two-dimensional magic clusters in the scattering of sound *Phys. Rev.* B **75** 241404

[15] Torrent D and Sánchez-Dehesa J 2007 Acoustic metamaterials for new acoustic devices *New J. Phys.* **9** 323

[16] Rayleigh J 1945 *Theory of Sound* (New York: Courier Dover)

[17] Berryman J G 1992 Single-scattering approximations for coefficients in Biot's equations of poroelasticity *J. Acoust. Soc. Am.* **91** 551

[18] Cummer S A and Schurig D 2007 One path to acoustic cloaking *New J. Phys.* **9** 45

[19] Leonhardt U 2006 Optical conformal mapping *Science* **312** 1777

[20] Pendry J B, Schurig D and Smith D R 2006 Controlling electromagnetic fields *Science* **312** 1780

[21] de Hoop A T 1995 *Handbook of Radiation and Scattering of Waves* (New York: Academic)

[22] Wood A B 1941 *Textbook of Sound* (New York: Macmillan)

[23] Ishimaru A 1978 *Wave Propagation ans Scattering in Random Media* (New York: Academic)

[24] Twersky V 1951 Sound scattering by solid cylinders and spheres *J. Acoust. Soc. Am.* **24** 42
[25] Chen Y Y and Ye Z 2001 Acoustic attenuation by two-dimensional arrays of rigid cylinders *Phys. Rev. Lett.* **87** 184301
[26] Waterman P C 1969 New formulation of acoustic scattering *J. Acoust. Soc. Am.* **45** 1417
[27] Faran J J 1951 Sound scattering by solid cylinders and spheres *J. Acoust. Soc. Am.* **23** 405
[28] Chin S K, Nicorovici N A and McPhedran R C 1994 Green's function and lattice sums for electromagnetic scattering by a square array of cylinders *Phys. Rev.* E **49** 4590
[29] Monzon J C and Damaskos N J 1986 *IEEE Trans. Antennas and Propag.* **AP-34** 1243